EXTENDED REPORT

Identi cation of microRNA-221/222 and microRNA-323-3p association with rheumatoid arthritis via predictions using the human tumour necrosis factor transgenic mouse model

Ioannis Pandis,[1] Caroline Ospelt,[2,3] Niki Karagianni,[1,4] Maria C Denis,[4] Martin Reczko,[5] Carme Camps,[6] Artemis G Hatzigeorgiou,[5] Jiannis Ragoussis,[6,7] Steffen Gay,[2,3] George Kollias[1]

► Additional supplementary materials are published online only. To view these files please visit the journal online (http://dx.doi.org/10.1136/annrheumdis-2011-200803)

[1]Institute of Immunology, Biomedical Sciences Research Centre 'Alexander Fleming', Vari, Greece
[2]Center of Experimental Rheumatology, University Hospital Zurich, Zurich, Switzerland
[3]Zurich Center of Integrative Human Physiology, Zurich, Switzerland
[4]Biomedcode Hellas SA, Vari, Greece
[5]Institute of Molecular Oncology, Biomedical Sciences Research Centre 'Alexander Fleming', Vari, Greece
[6]The Wellcome Trust Centre for Human Genetics, University of Oxford, Oxford, UK
[7]Institute of Molecular Biology and Genetics, Biomedical Sciences Research Centre, Vari, Greece

Correspondence to
George Kollias, Biomedical Sciences Research Centre 'Alexander Fleming', Institute of Immunology, Vari 16672, Greece; kollias@fleming.gr

Accepted 23 March 2012

ABSTRACT

Objective To identify novel microRNA (miR) associations in synovial fibroblasts (SF), by performing miR expression profiling on cells isolated from the human tumour necrosis factor (TNF) transgenic mouse model (TghuTNF, Tg197) and patients biopsies.

Methods miR expression in SF from TghuTNF and wild-type (WT) control mice were determined by miR deep sequencing (miR-seq) and the arthritic profile was established by pairwise comparisons. Quantitative PCR analysis was utilised for profile validation, miR and gene quantitation in patient SF. Dysregulated miR target genes and pathways were predicted via bioinformatic algorithms and validated using gain-of-function coupled with reporter assay experiments.

Results miR-seq demonstrated that TghuTNF-SF exhibit a distinct pathogenic profile with 22 significantly upregulated and 30 significantly downregulated miR. Validation assays confirmed the dysregulation of miR-223, miR-146a and miR-155 previously associated with human rheumatoid arthritis (RA) pathology, as well as that of miR-221/222 and miR-323-3p. Notably, the latter were also found significantly upregulated in patient RA SF, suggesting for the first time their association with RA pathology. Bioinformatic analysis suggested Wnt/cadherin signalling as a putative pathway target. miR-323-3p overexpression was shown to enhance Wnt pathway activation and decrease the levels of its predicted target β-transducin repeat containing, an inhibitor of β-catenin.

Conclusions Using miR-seq-based profiling in SF from the TghuTNF mouse model and validations in RA patient biopsies, the authors identified miR-221/222 and miR-323-3p as novel dysregulated miR in RA SF. Furthermore, the authors show that miR-323-3p is a positive regulator of WNT/cadherin signalling in RA SF suggesting its potential pathogenic involvement and future use as a therapeutic target in RA.

The multifactorial and complex molecular pathogenesis of rheumatoid arthritis (RA) creates hurdles in the understanding and treatment of this debilitating disease. Animal models of RA have been essential in overcoming patient heterogeneity, thus aiding basic understanding of biological mechanisms, identification and validation of novel pathogenic pathways and evaluation of diagnostic and therapeutic agents.[1] Neverthless, despite all efforts to date, the aetiology and comprehensive therapy of RA still remains elusive, warranting further study into its molecular mechanisms.

MicroRNA (miR), a class of small non-coding RNA molecules, act as post-transcriptional regulators and are involved in a plethora of cellular functions. They function predominantly by silencing target genes by binding to the 3′ untranslated region of their messenger RNA, in a sequence-specific manner, inhibiting mRNA translation or inducing mRNA degradation.[2] miR are highly abundant and show high stability in biological fluids, with changes in their levels correlating with disease prognosis and/or activity, nominating these molecules as valuable disease biomarkers.[3] In addition, miR have attracted a great deal of attention as potential therapeutic targets, as the sequence-specific mode in which they act allows the simultaneous targeting of multiple target genes, often members of the same biological pathway(s).[4] In the context of RA, miR-155, miR-146a, miR-223, miR-16 and miR-132 have been found to be dysregulated in patient peripheral blood mononuclear cells and various biological fluid samples including synovial fluid and plasma, providing a putative diagnostic potential.[5 6]

A key cell type mediating RA pathogenesis is the synovial fibroblast (SF), with current concepts proposing that therapeutics targeting RA SF could act synergistically with existing approaches leading to more favourable outcomes.[7] Therefore, a better understanding of the molecular changes occurring in RA SF is paramount for the generation of targeted therapeutics. miR perturbations have been reported in RA patient SF including the overexpression of miR-155, miR-146a and miR-203, and the underexpression of miR-124a.[8–10]

In this study, we hypothesised that additional perturbations in RA SF miR expression are currently masked by the heterogeneity present in patient genetic backgrounds and treatment regimes. To overcome this limitation, we used the TghuTNF mouse, a well-established mouse model of human RA that due to human tumour necrosis factor (TNF) deregulated expression develops spontaneous arthritis characterised by the infiltration of

inflammatory cells, synovial hyperplasia, cartilage destruction and bone erosion, closely resembling human pathology.[11] The development of full pathology in these mice is not dependent on haematopoietic TNFRI,[12] but interestingly is mediated by the direct activation of TNFR1 on SF.[13] Therefore, aiming to identify novel miR associated with the arthritic phenotype of RA SF we performed miR expression profiling on TghuTNF-SF and validated the results on human RA SF.

MATERIALS AND METHODS

Mice

TghuTNF mice were generated as previously described.[11] All mice were bred and maintained on a mixed CBA×C57BL/6J genetic background in the animal facilities of the Biomedical Sciences Research Center (BSRC) Alexander Fleming under specific pathogen-free conditions. All mice were used in accordance with the guidance of the Institutional Animal Care and Use Committee of BSRC Alexander Fleming.

Mouse and human cell isolation and culturing

Primary mouse SF were isolated from fully diseased 8-week-old TghuTNF and wild-type (WT) littermate mice (two mice per genotype were used for the miR deep sequencing (miR-seq) experiment and five to eight mice per genotype were used for profile validation) and cultured for three passages as previously described.[14] The cell purity of all preparations, was accessed via FACS. Representative profiles of the two TghuTNF and two WT SF cultures used for the miR-seq experiment are shown in supplementary figure S1 (available online only). Human RA and osteoarthritis (OA) SF were isolated and cultured as previously described.[10] Synovial tissue specimens were obtained during synovectomy or joint replacement surgery from patients with RA and patients with OA, after informed consent was obtained from all patients. The local ethics committee approved the study. All RA patients fulfilled the American College of Rheumatology criteria for the classification of RA.[15] All experiments using human cells were performed with SF in passages 4–7.

RNA isolation

Total RNA was isolated from cultured mouse and human cells using the miRVana miR isolation kit (Ambion) according to the manufacturer's protocol.

MiR-seq and miR expression profile generation

MiR deep sequencing

MiR-seq was performed on RNA from SF isolated from two TghuTNF and two WT littermate mice. Libraries were prepared as follows: the 20–30 and 70–100 nucleotide fractions were isolated from 10 µg of total RNA after being run in a 15% urea-TBE gel (Invitogen) for 1 h. The RNA contained on the excised gel bands was eluted in 300 µl of 0.3M NaCl solution during 4 h at room temperature and constant rotation. The elute was separated from the gel debris through a Spin-X-column (Fisher) and RNA was precipitated by adding 750 µl of 100% ethanol and 3 µl of glycogen (Ambion) (1 mg/ml) and incubating for 30 min at −80°C. The precipitated RNA was centrifuged at 14 000 rpm for 25 min at 4°C, washed with 75% ethanol and resuspended in 5.7 µl of RNAse-free water. A 5′ adaptor was ligated to the RNA in a reaction containing the full amount of RNA recovered from the last step, 1.3 µl of SRA 5′ adaptor (Illumina), 1 µl T4 RNA ligase (10 U/µl) (Promega), 1 µl 10X T4 RNA ligase reaction buffer (Promega) and 1 µl RNAseOUT (Invitrogen). The reaction was incubated at 20°C in a thermal cycler for 6 h. The resulting product was run on a 15% urea-TBE gel (Invitrogen) and the band corresponding to 40–60 nucleotides was excised. The 5′ ligated RNA was eluted and precipitated as described before and finally resuspended in 6.4 µl of RNAse-free water. A 3′ adaptor was added to these molecules in a reaction containing the entire 5′ ligated RNA recovered from the last step, 0.6 µl of SRA 3′ adaptor (Illumina), 1 µl T4 RNA ligase (10 U/µl; Promega), 1 µl 10X T4 RNA ligase (Promega) and 1 µl RNAseOUT (Invitrogen). The reaction was incubated at 20°C in a thermal cycler for 6 h. The product obtained was run on a 10% urea-TBE gel (Invitrogen) and the band corresponding to 70–90 nucleotides was excised. The 5′ and 3′ ligated RNA was eluted and precipitated as described before and finally resuspended in 4.5 µl of RNAse-free water. In order to synthesise single-stranded DNA from this material, 0.5 µl of SRA RT-primer (Illumina) were added and the mixture was incubated at 65°C for 10 min. This was complemented with 2 µl of 5X first strand buffer, 1 µl 100 mM dithiothreitol, 0.5 µl RNAseOUT (all from the Superscript II reverse transcription kit (Invitrogen) and 0.5 µl 12.5 mM dNTP mix (BioLine)) and incubated at 48°C for 3 min. After adding 1 µl of Superscript II retrotranscriptase (Invitrogen), the reaction was incubated at 44°C for 1 h. A PCR reaction was then set up with the resultant product and 0.5 µl GX1 primer, 0.5 µl GX2 primer (both from Illumina), 0.5 µl 25mM dNTP mix (BioLine), 10 µl 5X cloned Phu buffer, 0.5 µl Phu polymerase (both from NEB) and 28 µl RNAse-free water. The cycling conditions were as follows: one cycle of 98°C for 30 s; 15 cycles of 98°C for 10 s, 60°C for 30 s and 72°C for 15 s; one cycle of 72°C for 10 min. The PCR product was purified by running it on a 10% TBE-polyacrylamide gel electrophoresis gel for 35 min. The band around 90 bp was excised and eluted on 100 µl of 1X elution buffer 2 (NEB) for 2 h at room temperature and at constant rotation. The elute was separated from the gel debris through a Spin-X-column (Fisher) and DNA was precipitated by adding 1 µl of glycogen (1 mg/ml; Ambion), 10 µl 3M sodium acetate (Ambion) and 325 µl of −20°C100% ethanol and centrifuging at 14 000 rpm for 20 min. After a wash with 70% ethanol, the DNA was vacuum dried and resuspended in 10 µl water. The libraries were sequenced using an Illumina GA II machine according to the manufacturer's standard protocols at 36 bp read length.

Alignment algorithm

Our short sequence alignment method is based on a de Bruijn graph representation of the reference collection of known miR sequences.[16] This collection contained all murine major and minor (or star) mature miR as defined in mirBase release 15.0, giving a total of 707 sequences. All 9mers occurring in each reference sequence and its reverse complement were stored in a hash table together with an identifier for the reference sequence and its start position within the sequence. For each read, all valid paths through the reference sequences were collected, allowing for up to two sequence edits (mismatches, insertions or deletions).

TghuTNF-SF miR expression pro le generation

For miR expression profile generation miR transcript abundance (sequencing reads) was used as a measure of expression. To allow pairwise comparisons, as a common practice, miR read numbers in each sample were normalised to the total reads per million. All miR that had less than six reads in any of the samples were considered as not being expressed and were discarded. Subsequently, expression fold change (FC) was calculated by dividing the average TghuTNF reads by the average WT reads. miR showing a FC of less than 1.5 were also discarded. Significant

differences in the expression of the remaining 141 miR between the two groups were determined using an unpaired two-sided t test, on the $\log_2$-transformed reads, as proposed by Creighton *et al*.[17] miR with a p value of less than 0.05, FC greater than 1.5 and a false discovery rate of less than 5% (calculated according to Storey and Tibshirani)[18] were considered significantly dysregulated. All sequencing data have been deposited on gene expression omnibus with ID GSE31667.

Profile validation and human patient SF miR and gene expression quantitation

Profile validation was performed on TghuTNF (n≥5) and WT (n≥5) SF isolated in independent experiments, using quantitative real-time PCR based TaqMan MiR assays (Applied Biosystems) according to the manufacturer's instructions, on a Chromo4 real-time PCR detection system (Bio-Rad Laboratories). Small nuclear RNA U6 was used as an endogenous control for normalisation purposes and expression FC were calculated using the ΔΔC(t) method.[19] Samples with a C(t) greater than 35 were considered below detection.

Human patient quantitations of miR, casein kinase I isoform alpha (CSNK1A1), β-transducin repeat containing (BTRC) and glycogen synthase kinase 3 beta (GSK3B) were performed on RA SF and OA SF as a control, using the same quantitative reverse transcription PCR assays described above, on a 7500 real-time PCR system (Applied Biosystems). let-7a miR was used as an endogenous control for miR measurements while ribosomal 18S levels were used for mRNA measurements. Differences in expression were assessed using the ΔC(t) method, as previously described.[9 10] For the detection of CSNK1A1, BTRC and GSK3B, SYBR dye and the following primer pairs were used: CSNK1A1 forward (fw) CGGCGAGGAAGTGGCAGTGA, reverse (rev) TGGGGATGCCTGGCCTTCTGA; BTRC fw CCCGTGCTCCTGCAGGGACA, rev CGGAATGCTCCACAAGGGTCCG; GSK3B transcript variant 1 fw TCAGGAGTGCGGGTCTTCCGA, rev CAGTGCAATTGCCTCCGGTGGA; GSK3B transcript variant 2 fw TTGGACTAAGGTCTTCCGACCCCG, rev CAGTGCAATTGCCTCCGGTGGA.

Bioinformatics

MiR expression clustering and heatmap generation

Pearson correlation-based clustering and heatmap generation of miR expression profiles was calculated using the made4 package for the the R statistics environment.[20]

MiR target prediction and pathway analysis

Human and mouse miR target predictions were performed using the DIANA microT and TargetScan algorithms.[21 22] The g:Profiler tool was used for all gene ID conversion purposes[23] and the Panther repository was used for pathway enrichment analysis.[24]

For each species miR targets, we combined the unions of the two algorithm outputs, which weight species conservation of predicted targets differentially, producing more sensitive target lists. By comparing the mouse and human gene target lists we generated lists of conserved, mouse-specific and human-specific targets, for each miR (see supplementary excel file, available online only). Pathway enrichment analysis was performed on the conserved lists, using the species-specific lists as controls to exclude random enrichment, against the default homo sapiens reference gene list provided by Panther. Pathways with a p value less than 0.001 were considered significantly enriched.

MiR overexpression and WNT reporter assays

Co-transfections of a human cell line with a WNT reporter plasmid and miR precursors (pre-miR) were performed to clarify miR and pathway relationship, whereas transfections of RA SF with pre-miR were used to assess the regulatory potential of miR on target genes. HEK 293T cells were used for reporter plasmid transfections (a kind gift from Dr Hatzis, Fleming, Athens). Pre-miR miRNA precursors (Ambion) were used for miR overexpression. The M50 Super 8x TOPFlash[25] wnt reporter plasmid was purchased from Addgene and a CMV/green fluorescent protein (GFP)-expressing plasmid was used to control transfection efficiency. The Lipofectamine 2000 (Invitrogen) reagent was used for plasmid and pre-miR transfections and the Steady-Glo luciferase assay system (Promega UK, Southampton, UK) was used for luciferase activity quantitation. Luminescence and GFP fluorescence were measured on an Infinite M200 multimode reader (Tecan). Assays were performed according to the pre-miR miRNA precursor guidelines.

Briefly, for each transfection 10^4 HEK 293T cells were seeded in one well of Corning 96-well flat clear bottom white polystyrene TC plates and transfected using the lipid-mediated forward co-transfection method with 50 nM pre-miR (25 nM of each miR in the case of miR-221/222), 40 ng Super 8x TOPFlash plasmid and 4 ng CMV/GFP for 48 h. After 48 h, the WNT pathway was activated by treating the cells with 10 mM LiCl for 16 h, followed by cell lysis and quantitation of luminescence and fluorescence. Each miR, including the control, was transfected four times in each experiment and each experiment was repeated three times.

For transfection of RA SF with pre-miR, cells were seeded at 50×10^4/well in 12-well plates and transfected with 50 nM pre-miR 323-3p or pre-miR negative control (Ambion) using lipofectamine 2000 (Invitrogen). Medium was changed after 24 h, and cells were lysed with QIAzol lysis reagent (Ambion) 72 h after transfection. Total RNA was isolated using the miRVana miR isolation kit (Ambion) and the expression of target genes was measured with the 7500 real-time PCR system as described above.

Statistics

Statistical analyses were performed using GraphPad Prism. For profile validation purposes, significant ($p<0.05$) FC between the two groups were computed using a one-sample t test. Pearson's correlation coefficient was used as similarity measure of miR-seq and quantitative PCR-based FC, after Gaussian distribution was checked using the Shapiro–Wilk's test.

Significant differences ($p<0.05$) between RA and OA SF miR expression were assessed using unpaired two-tailed t tests on quantitative PCR ΔC(t) values, after Gaussian distribution was checked using the Kolmogorov–Smirnov test for n=5 or Shapiro–Wilk's for n≥6.

RESULTS

TghuTNF-SF exhibit a distinct pathogenic miR expression profile overlapping with that of RA patient SF

The miR expression profiles of SF isolated from two fully diseased 8-week-old TghuTNF and two healthy WT littermate mice were determined by miR-seq. Pairwise significance analysis of the two profiles showed that 22 miR are upregulated and 30 miR downregulated in TghuTNF-SF, FC greater than 1.5, p value less than 0.05 and false discovery rate less than 5% (figure 1A and supplementary table S1, available online only). All sequencing data have been deposited on gene expression

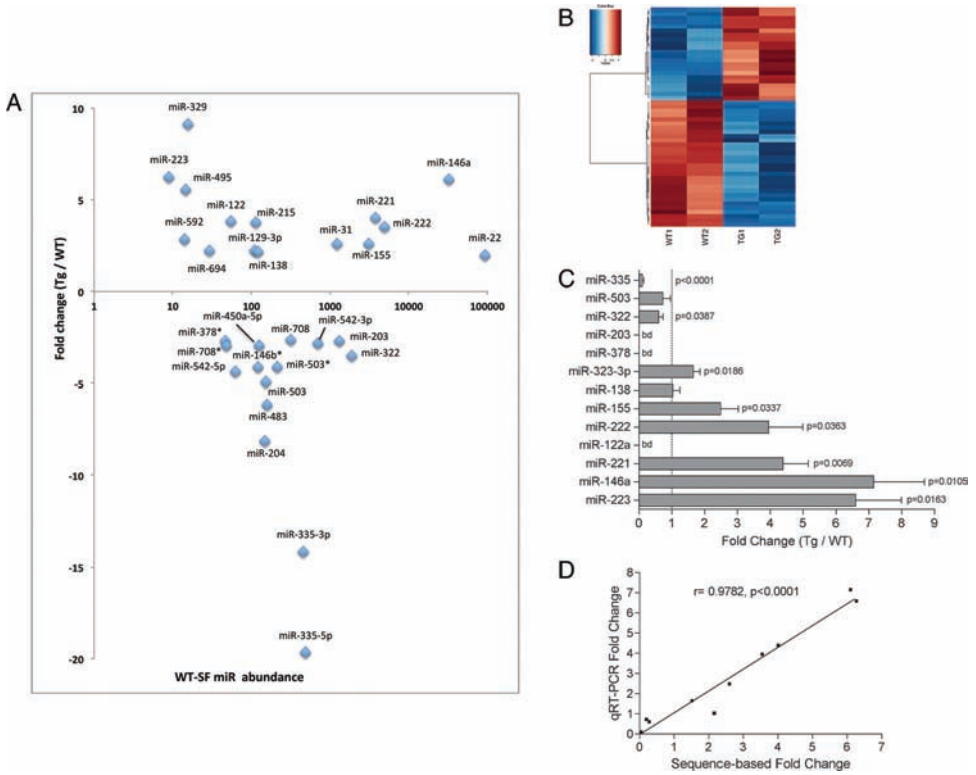

Figure 1 The TghuTNF-synovial broblast (SF) microRNA (miR) sequence-based expression pro le. Sequence-based expression pro le of signi cantly dysregulated miR in TghuTNF-SF (n=2) compared with wild-type (WT) SF (n=2). (A) Top 15 upregulated and downregulated miR. Fold change (Tg/WT) plotted on the y-axis and miR abundance in WT SF is plotted on the x-axis, providing both a measure of dysregulation and expression. (B) Pearson correlation coef cient-based clustering heat map representation of the expression pro le, showing that TghuTNF-SF express a distinct pathogenic pro le compared with WT SF. (C) Average fold change in miR expression in TghuTNF versus WT littermate SF (data from ve to eight independent experiments combined). Levels were determined using TaqMan miR assays. Fold change was calculated using the ΔΔCt method. All miR levels were normalised to U6 small nuclear RNA. Error bars represent ±SEM. p Values calculated using a onesample t test. bd, Below detection (C(t)>35). (D) Pearson correlation between miR fold change determined by sequencing and quantitative reverse transcription PCR, showing that the sequence-based expression pro le is valid and quantitative (r=0.9782, p<0.0001, n=10).

omnibus with ID GSE31667. Profile validation was performed on a panel of 13 randomly selected miR via quantitative PCR, on independently isolated pairs of SF (n≥5). The upregulation of miR-223, miR-146a, miR-155, miR-221, miR-222 and miR-323-3p, and the downregulation of miR-322 and miR-335 in TghuTNF-SF was confirmed, while the dysregulation of miR-138 and miR-503 was not, and miR-122a, miR-203 and miR-378 levels were below the assay detection capacity (figure 1C and supplementary table S1, available online only).

The validity and quantitative capacity of the sequence-based expression profile was further underlined by the significant positive correlation (r=0.9782, p<0.0001, n=10) of miR-seq and quantitative PCR-based FC, determined by Pearson correlation analysis (figure 1D).

Current literature on the association of miR with RA SF report miR-155, miR-146a and miR-203 overexpression, and reduced levels of miR-124a in RA SF compared with OA SF.[8–10] Our results show that miR-203 is downregulated in the TghuTNF-SF profile, but was below detection in quantitative PCR validation assays (figure 1A,C, supplementary tables S1 and S2, available online only). In addition, miR-124 transcripts could not be detected in any of the four samples sequenced (data not shown). In contrast, miR-155 and miR-146a are indeed overexpressed in TghuTNF-SF (figure 1A,C and supplementary table S2, available online only), indicating that the profile overlaps with the current RA patient SF findings.

TghuTNF-SF and RA SF miR expression profile comparison identifies miR-221/222 and miR-323-3p association with RA SF

Next we examined our hypothesis that additional miR perurbations are shared between TghuTNF-SF and RA SF. To this end, the validated mouse profile miR were quantitated via quantitative PCR in patient RA SF (n=8) using OA SF (n=8) as a control.

No significant differences were found in miR-223, miR-335, miR-424 (homologue of mouse miR-322) or notably miR-146a expression, which has previously been reported to be altered in RA SF.[10] This incomplete penetrance of miR-146a may be due to heterogeneity present in patient samples. Interestingly, miR-155 dysregulation was verified and most notably we found that miR-221, miR-222 and miR-323-3p are significantly overexpressed in RA SF, establishing for the first time their association with RA (figure 2, supplementary table S3, available online only).

In-silico predictions of miR-221/222 and miR-323-3p conserved targets and pathways

Subsequently, we investigated the putative functional role of the newly associated miR. To this end, pathway enrichment analysis was performed using Panther[24] on sensitive lists (see Materials and methods section, and supplementary excel file, available online only) of conserved miR gene targets in humans and mice, predicted by two major target prediction algorithms, namely DIANA microT and TargetScan.[21 22] Human and mouse-specific target lists (see supplementary excel file, available online only)

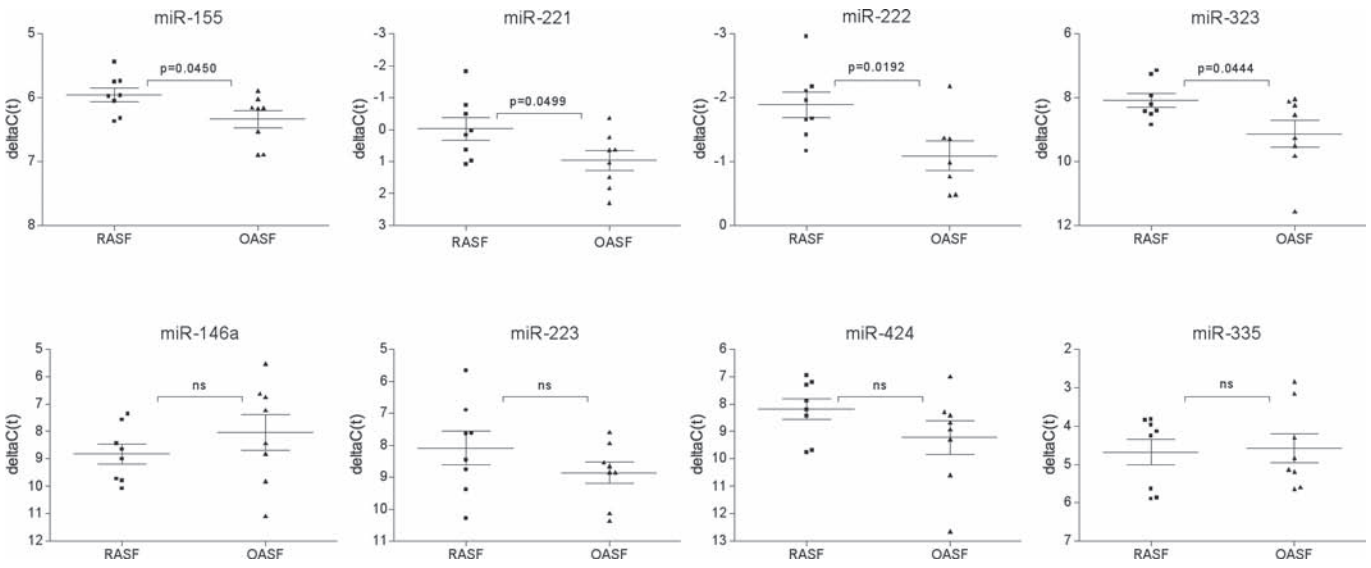

Figure 2 MicroRNA (miR) dysregulated in rheumatoid arthritis (RA) versus osteoarthritis (OA) patient synovial broblasts (SF). Expression differences of miR in RA (n=8) and OA (n=8) SF. Levels were determined using TaqMan miR assays. Relative expression differences were calculated using the ΔC(t) method. All miR levels were normalised to let-7a miR. Bars represent the mean. p Values were calculated using an unpaired t test. ns, not signi cant.

were used as controls, to exclude enrichment due to redundancy often observed in these types of analyses.

MiR-221 and miR-222 were studied simultaneously, as they are a co-expressed cluster of miR, possessing identical 5′ seed regions targeting the same genes. The miR-221/222 conserved target gene list (978 genes) showed a significant enrichment (p<0.001) in 11 pathways, whereas three pathways enriched in the mouse-specific target list (1420 genes) and the human-specific list (2040 genes) showed no significant enrichment in any pathways (table 1 and supplementary excel file, available online only). The miR-323-3p analysis revealed a significant enrichment in 18 pathways in the conserved target list (1711 genes), no significant enrichment in the mouse-specific list (1326 genes) and one in the human-specific list (3077 genes; table 2 and supplementary excel file, available online only). All target genes involved in enriched pathways are provided (supplementary excel file, available online only).

Interestingly, pathways previously associated with RA pathogenesis, such as wnt,[26 27] cadherin,[28] angiogenesis,[29] Ras,[30] PI3K,[31] PDGF,[32] T-cell activation[33] and integrin[29] pathways were enriched in both miR target lists, implying that the newly identified miR may modulate more than one key arthritogenic pathway.

Table 1 Pathway enrichment analysis of miR-221/222 conserved predicted target genes

Pathway	Reference gene number† (total: 19 911)	Conserved target gene number‡ (total: 978)	Expected number§	Enrichment p value
Wnt signalling pathway	317	46	15.57	2.03E-10
Cadherin signalling pathway	147	26	7.22	4.34E-08
Angiogenesis	191	27	9.38	1.76E-06
Alzheimer s disease-presenilin pathway	122	18	5.99	5.22E-05
Ras pathway	79	14	3.88	5.30E-05
PI3 kinase pathway	115	16	5.65	2.54E-04
Metabotropic glutamate receptor group II pathway	51	10	2.51	2.75E-04
Muscarinic acetylcholine receptor 2 and 4 signalling pathway	62	11	3.05	3.21E-04
Metabotropic glutamate receptor group III pathway	73	12	3.59	3.46E-04
PDGF signalling pathway*	159	19	7.81	4.61E-04
T cell activation	102	14	5.01	6.84E-04

*Also enriched in mouse-speci c target gene list (p value=2.90e-04) (see supplementary excel le, available online only).
Number of human genes in Panther pathway.
Number of conserved target genes in Panther pathway
Expected number of conserved target genes based on list size.
miR, microRNA; PDGF, platelet-derived growth factor.

MiR-323-3p enhances Wnt/cadherin pathway activation

Pathway enrichment analysis indicated Wnt and cadherin signalling as the top pathways potentially affected by both miR-221/222 and miR-323-3p overexpression. Activation of wnt/cadherin signalling in RA has been reported and the constitutive upregulation of β-catenin, a common component of both pathways,[34] has been linked to the RA SF activated phenotype.[26–28 35 36] Accordingly, gain of function experiments showed that WNT reporter activity induced by lithium salt treatment[37] was significantly increased in HEK 293T cells overexpressing miR-323-3p (figure 3A). miR-221/222 overexpression showed no effect.

Interestingly, CSNK1A1, BTRC and GSK3B that are known mediators of the degradation of β-catenin,[38] were predicted targets of miR-323-3p (see supplementary excel file, available online only). Subsequent quantitative PCR determination of their expression levels showed that while CSNK1A1 expression was not significantly changed, both GSK3B transcript variants, GSK3Btr1 and GSK3Btr2, and BTRC expression was found significantly decreased in RA compared with OA SF (figure 3B).

To determine if BTRC and/or GSK3B are regulated by miR-323-3p, we overexpressed miR-323-3p in RA SF, which led to the significant decrease of BTRC mRNA, whereas neither of the GSK3B transcripts was affected (figure 3C). In addition, miR-323-3p and BTRC expression levels showed a significant inverse correlation in RA SF (r=−0.5336, p=0.037; figure 3D). Collectively these results suggest that miR-323-3p overexpression leads to

Table 2 Pathway enrichment analysis of miR-323-3p conserved predicted target genes

Pathway	Reference gene number* (total: 19911)	Conserved target gene number† (total: 1711)	Expected number‡	Enrichment p value
Wnt signalling pathway	317	69	27.24	8.98E-12
Cadherin signalling pathway	147	35	12.63	1.49E-07
Angiogenesis	191	37	16.41	7.61E-06
In ammation mediated by chemokine and cytokine signalling pathway	283	46	24.32	4.99E-05
Metabotropic glutamate receptor group II pathway	51	15	4.38	5.35E-05
Endothelin signalling pathway	91	21	7.82	6.56E-05
EGF receptor signalling pathway	135	27	11.6	7.28E-05
Metabotropic glutamate receptor group III pathway	73	18	6.27	9.47E-05
Axon guidance mediated by semaphorins	43	13	3.7	1.26E-04
Integrin signallling pathway	181	32	15.55	1.58E-04
PDGF signalling pathway	159	29	13.66	1.89E-04
Ras pathway	79	18	6.79	2.44E-04
T-cell activation	102	21	8.77	3.01E-04
Heterotrimeric G-protein signalling pathway-Gq alpha and Go alpha-mediated pathway	134	25	11.51	3.65E-04
Ubiquitin proteasome pathway	70	16	6.02	5.09E-04
Parkinson s disease	100	20	8.59	5.88E-04
Apoptosis signalling pathway	123	23	10.57	5.95E-04
GABA-B_receptor_II_ signalling	40	11	3.44	8.70E-04

*Number of human genes in Panther pathway.
Number of conserved targets genes in Panther pathway.
Expected number of conserved target genes based on list size.
EGR, endothelial growth factor; miR, microRNA; PDGF, platelet-derived growth factor.

enhanced activation of Wnt/cadherin pathways, partly by targeting BTRC in RA SF.

DISCUSSION

MiR have been proposed as potentially valuable targets in RA with current literature reporting the dysregulated expression of miR-223, miR-155, miR-146a and miR-16 in patient peripheral blood mononuclear cells and synovial fluid, reduced miR-132 levels in RA plasma and miR-155, miR-146a, miR-203 and miR-124a dysregulations in patient SF.[5 6 8–10] miR functional studies suggest a protective role for miR-155 in RA SF, as it has been shown to reduce matrix metalloproteinase 1 and matrix metalloproteinase 3 expression.[10] Conversely, in-vivo functional experiments using miR-155-deficient mice have indicated a pathogenic role for miR-155 in immune cells, as deficient mice are protected against antigen-driven arthritis, through the blockade of antigen-specific T-helper 17 polarisation and show reduced immune-mediated bone destruction in the serum-transfer model of arthritis by the partial inhibition of osteoclastogenesis.[39 40] Furthermore, despite miR-146a upregulation in various RA patient cell types suggesting a pathogenic role, in-vivo exogenous double-stranded miR-146a administration after the induction of auto-antigen-driven arthritis in mice, led to a decrease in bone erosion via the partial inhibition of osteoclastogenesis, with no effect on joint inflammation.[41]

Whereas studies on human patient samples are paramount in the direct identification of disease determinants and therapeutic targets, their heterogeneity as a result of diverse genetic backgrounds, environmental conditions and treatment regimes impedes this discovery process. Animal models of disease, such as the TghuTNF model, although not fully representing the heterogeneity seen in RA, do show pathogenic and therapeutic alignment with aspects of human disease, providing invaluable tools to overcome such hurdles due to their homogeneity and complete disease penetrance. Comparative studies utilising both sample types should thus be advantageous in the identification of novel pathogenic mechanisms or biomarkers.[1]

In this study, we overcame limitations possessed by patient heterogeneity by using the TghuTNF mouse. We focused on SF, which are key cells driving human RA pathology and can alone instigate full pathology in this mouse model.[12 13] By comparing the mouse and human arthritic profiles we found that they overlap and importantly we established a miR-221/222 and miR-323-3p association with RA SF. The TghuTNF-SF miR expression profile is provided here as a resource, which may contain further currently unidentified miR dysregulations associated with human pathology.

A search of the current literature did not identify any evidence to support a function for miR-323-3p, in contrast miR-221/222 is an established 'oncomiR' cluster overexpressed in various human cancers. The cluster mediates oncogenic transformation in cancer cells by enhancing cellular proliferation, inhibiting apoptosis and enhancing cellular migration.[42] These functions are also altered in RA SF,[43 44] suggesting that they may be regulated by miR-221/222 overexpression.

Furthermore, utilising in-silico target predictions and pathway enrichment analysis, we investigated putative target genes and pathways modified by the newly associated miR. Interestingly, the most significantly enriched pathways were Wnt and cadherin signalling. The importance of cadherin signalling in RA has been established, as cadherin-11 is necessary for the mounting of an inflammatory response by RA SF and maintenance of the correct architecture of the synovium.[28 36] In addition, the role of the Wnt pathway has also been initially highlighted by a study by Diarra *et al*,[26] as the inhibition of its key regulator Dickkopf-1 results in the reversal of the bone-destructive phenotype of TghuTNF mice and Dickkopf-1 was shown to be highly expressed in RA SF. Moreover, a recent study has further underscored this association of the WNT pathway in RA SF, by showing that the pathway activation is epigenetically controlled by the enhancer of zeste homologue 2.[27] These key pathways contributing to the pathogenic phenotype of RA SF converge at β-catenin.[34]

Notably, we show here that miR-323-3p enhances Wnt activation. In addition, miR-323-3p overexpression led to the decreased levels of the negative regulator of β-catenin, BTRC, implying that cadherin signalling may also be modulated. We propose that BTRC is only one of the perturbed Wnt/cadherin signalling components and that additional key molecules are also regulated by miR-323-3p and/or other miR dysregulated in RA SF. Jointly, these results propose the dysregulation of the Wnt/cadherin pathway as a potential pathogenic target of miR-323-3p in RA SF, and that intervention using miR-323-3p inhibitors may be of therapeutic value.

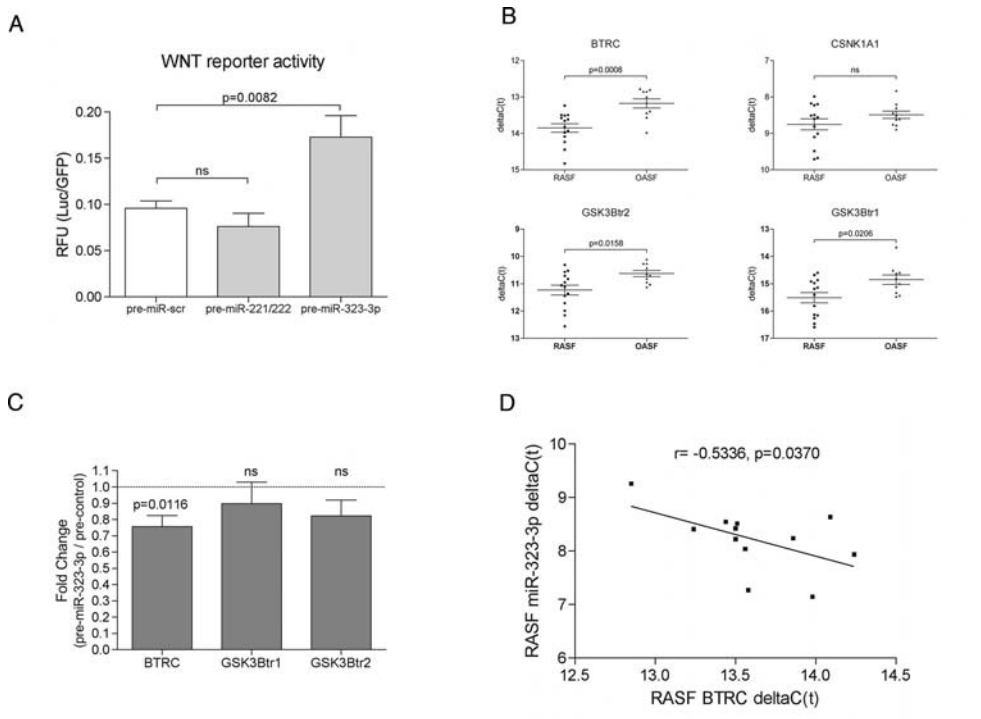

Figure 3 MicroRNA (miR)-323-3p overexpression, but not miR-221/222, enhances WNT pathway activation and decreases the levels of its predicted target β-transducin repeat containing (BTRC). (A) WNT reporter activity in HEK 293T cells transfected for 48 h with 50 nM miR precursor (pre-miR)-323-3p or 50 nM pre-miR-221/222 (25nM of each miR-221 and miR-222) or 50 nM pre-miR-scr (control). WNT activation was induced by treatment with 10 mM LiCl for 16 h. Luciferase activity was normalised for transfection ef ciency by green uorescent protein (GFP) expression and is presented as relative uorescence units (RFU). Results show that miR-323-3p, but not miR-221/222, enhances Wnt activation. Error bars represent ±SEM and n=12 transfection for each pre-miR. (B) Expression differences of casein kinase I isoform alpha (CSNK1A1), BTRC and glycogen synthase kinase 3 beta (GSK3B), negative regulators of β-catenin, in rheumatoid arthritis (RA) (n=14) and osteoarthritis (OA) (n=10) SF. Levels were determined by quantitative reverse transcription PCR (qRT PCR). Relative expression differences were calculated using the ΔC(t) method. All transcript levels were normalised to 18 s. (C), Expression differences of BTRC and GSK3B, in RA SF (n=7) transfected with 50 nM pre-miR-323-3p or 50 nM pre-miR-scr (control), showing that miR-323-3p overexpression decreases the levels of BTRC. Levels were determined by qRT PCR. Relative expression differences were calculated using the ΔΔC(t) method. All transcript levels were normalised to 18 s. Bars represent the mean. (D) Pearson correlation between miR-323-3p and BTRC expression in RA SF (n=12), showing a signi cant inverse correlation (r=−0.5336, p=0.037). p Values were calculated using an unpaired t test. ns, not signi cant.

Acknowledgements The authors would like to thank Dr Fotsis and Dr Christoforidis for discussions, Dr Moon for constructing the Super 8x TOPFlash plasmid, Dr Hatzis for providing cell lines and together with Dr Bertrand and Dr Dell'accio providing invaluable technical advice. Finally, IP would like to dedicate the paper to the late Mrs. M. Batten for continuous moral support.

Funding This project was funded by the Masterswitch Project (HEALTH-F2-2008–223404), EURO-RA RTN (HPRN-CT-2002-00255) and IMI BtCure (grant agreement no. 115142) grants to GK and SG. JR was supported by the Wellcome Trust grant 075491/Z/04. SG also received funding from IAR-EPALINGES.

Contributors IP performed experiments, analysed data and wrote the manuscript. CO performed experiments and analysed data. NK and MCD designed and performed experiments and wrote the manuscript. MR designed and analysed data. CC performed experiments. AH, JR and SG designed experiments and analysed data. GK designed experiments, analysed data, wrote the manuscript. All authors revised the manuscript. IP, CO, MR and GK are guarantors.

Ethics approval The local ethics committee approved the study.

Patient consent Obtained.

Competing interests None.

Provenance and peer review Not commissioned; externally peer reviewed.

REFERENCES

1. **Kollias G**, Papadaki P, Apparailly F, *et al*. Animal models for arthritis: innovative tools for prevention and treatment. *Ann Rheum Dis* 2011;**70**:1357–62.
2. **Bartel DP**. MicroRNAs: genomics, biogenesis, mechanism, and function. *Cell* 2004;**116**:281–97.
3. **Wang Y**, Li Z, He C, *et al*. MicroRNAs expression signatures are associated with lineage and survival in acute leukemias. *Blood Cells Mol Dis* 2010;**44**:191–7.
4. **Montgomery RL**, van Rooij E. MicroRNA regulation as a therapeutic strategy for cardiovascular disease. *Curr Drug Targets* 2010;**11**:936–42.
5. **Murata K**, Yoshitomi H, Tanida S, *et al*. Plasma and synovial fluid microRNAs as potential biomarkers of rheumatoid arthritis and osteoarthritis. *Arthritis Res Ther* 2010;**12**:R86.
6. **Pauley KM**, Satoh M, Chan AL, *et al*. Upregulated miR-146a expression in peripheral blood mononuclear cells from rheumatoid arthritis patients. *Arthritis Res Ther* 2008;**10**:R101.
7. **Bartok B**, Firestein GS. Fibroblast-like synoviocytes: key effector cells in rheumatoid arthritis. *Immunol Rev* 2010;**233**:233–55.
8. **Kawano S**, Nakamachi Y. miR-124a as a key regulator of proliferation and MCP-1 secretion in synoviocytes from patients with rheumatoid arthritis. *Ann Rheum Dis* 2011;**70** (Suppl 1):i88–91.
9. **Stanczyk J**, Ospelt C, Karouzakis E, *et al*. Altered expression of microRNA-203 in rheumatoid arthritis synovial fibroblasts and its role in fibroblast activation. *Arthritis Rheum* 2011;**63**:373–81.
10. **Stanczyk J**, Pedrioli DM, Brentano F, *et al*. Altered expression of MicroRNA in synovial fibroblasts and synovial tissue in rheumatoid arthritis. *Arthritis Rheum* 2008;**58**:1001–9.
11. **Keffer J**, Probert L, Cazlaris H, *et al*. Transgenic mice expressing human tumour necrosis factor: a predictive genetic model of arthritis. *EMBO J* 1991;**10**:4025–31.
12. **Blüml S**, Binder NB, Niederreiter B, *et al*. Antiinflammatory effects of tumor necrosis factor on hematopoietic cells in a murine model of erosive arthritis. *Arthritis Rheum* 2010;**62**:1608–19.
13. **Armaka M**, Apostolaki M, Jacques P, *et al*. Mesenchymal cell targeting by TNF as a common pathogenic principle in chronic inflammatory joint and intestinal diseases. *J Exp Med* 2008;**205**:331–7.

14. **Armaka M**, Gkretsi V, Kontoyiannis D, et al. A standardized protocol for the isolation and culture of normal and arthritogenic murine synovial fibroblasts. Protocol Exchange 2009. doi:10.1038/nprot.2009.102.
15. **Arnett FC**, Edworthy SM, Bloch DA, *et al*. The American Rheumatism Association 1987 revised criteria for the classification of rheumatoid arthritis. *Arthritis Rheum* 1988;**31**:315–24.
16. **Pevzner PA**, Tang H, Waterman MS. An Eulerian path approach to DNA fragment assembly. *Proc Natl Acad Sci U S A* 2001;**98**:9748–53.
17. **Creighton CJ**, Reid JG, Gunaratne PH. Expression profiling of microRNAs by deep sequencing. *Brief Bioinformatics* 2009;**10**:490–7.
18. **Storey JD**, Tibshirani R. Statistical significance for genomewide studies. *Proc Natl Acad Sci U S A* 2003;**100**:9440–5.
19. **Livak KJ**, Schmittgen TD. Analysis of relative gene expression data using real-time quantitative PCR and the 2(-Delta Delta C(T)) Method. *Methods* 2001;**25**:402–8.
20. **Culhane AC**, Thioulouse J, Perrière G, *et al*. MADE4: an R package for multivariate analysis of gene expression data. *Bioinformatics* 2005;**21**:2789–90.
21. **Friedman RC**, Farh KK, Burge CB, *et al*. Most mammalian mRNAs are conserved targets of microRNAs. *Genome Res* 2009;**19**:92–105.
22. **Maragkakis M**, Vergoulis T, Alexiou P, *et al*. DIANA-microT Web server upgrade supports Fly and Worm miRNA target prediction and bibliographic miRNA to disease association. *Nucleic Acids Res* 2011;**39**:W145–8.
23. **Reimand J**, Kull M, Peterson H, *et al*. g:Profiler – a web-based toolset for functional profiling of gene lists from large-scale experiments. *Nucleic Acids Res* 2007;**35**:W193–200.
24. **Thomas PD**, Kejariwal A, Guo N, *et al*. Applications for protein sequence-function evolution data: mRNA/protein expression analysis and coding SNP scoring tools. *Nucleic Acids Res* 2006;**34**:W645–50.
25. **Veeman MT**, Slusarski DC, Kaykas A, *et al*. Zebrafish prickle, a modulator of noncanonical Wnt/Fz signaling, regulates gastrulation movements. *Curr Biol* 2003;**13**:680–5.
26. **Diarra D**, Stolina M, Polzer K, *et al*. Dickkopf-1 is a master regulator of joint remodeling. *Nat Med* 2007;**13**:156–63.
27. **Trenkmann M**, Brock M, Gay RE, *et al*. Expression and function of EZH2 in synovial fibroblasts: epigenetic repression of the Wnt inhibitor SFRP1 in rheumatoid arthritis. *Ann Rheum Dis* 2011;**70**:1482–8.
28. **Lee DM**, Kiener HP, Agarwal SK, *et al*. Cadherin-11 in synovial lining formation and pathology in arthritis. *Science* 2007;**315**:1006–10.
29. **Koch AE.** Review: angiogenesis: implications for rheumatoid arthritis. *Arthritis Rheum* 1998;**41**:951–62.
30. **Trabandt A**, Aicher WK, Gay RE, *et al*. Expression of the collagenolytic and Ras-induced cysteine proteinase cathepsin L and proliferation-associated oncogenes in synovial cells of MRL/l mice and patients with rheumatoid arthritis. *Matrix* 1990;**10**:349–61.
31. **Kim KW**, Cho ML, Park MK, *et al*. Increased interleukin-17 production via a phosphoinositide 3-kinase/Akt and nuclear factor kappaB-dependent pathway in patients with rheumatoid arthritis. *Arthritis Res Ther* 2005;**7**:R139–48.
32. **Rosengren S**, Corr M, Boyle DL. Platelet-derived growth factor and transforming growth factor beta synergistically potentiate inflammatory mediator synthesis by fibroblast-like synoviocytes. *Arthritis Res Ther* 2010;**12**:R65.
33. **Burger D**, Rezzonico R, Li JM, *et al*. Imbalance between interstitial collagenase and tissue inhibitor of metalloproteinases 1 in synoviocytes and fibroblasts upon direct contact with stimulated T lymphocytes: involvement of membrane-associated cytokines. *Arthritis Rheum* 1998;**41**:1748–59.
34. **Nelson WJ**, Nusse R. Convergence of Wnt, beta-catenin, and cadherin pathways. *Science* 2004;**303**:1483–7.
35. **Xiao CY**, Pan YF, Guo XH, *et al*. Expression of β-catenin in rheumatoid arthritis fibroblast-like synoviocytes. *Scand J Rheumatol* 2011;**40**:26–33.
36. **Chang SK**, Noss EH, Chen M, *et al*. Cadherin-11 regulates fibroblast inflammation. *Proc Natl Acad Sci U S A* 2011;**108**:8402–7.
37. **Klein PS**, Melton DA. A molecular mechanism for the effect of lithium on development. *Proc Natl Acad Sci U S A* 1996;**93**:8455–9.
38. **Morikawa T**, Kuchiba A, Yamauchi M, *et al*. Association of CTNNB1 (beta-catenin) alterations, body mass index, and physical activity with survival in patients with colorectal cancer. *JAMA* 2011;**305**:1685–94.
39. **Blüml S**, Bonelli M, Niederreiter B, *et al*. Essential role of microRNA-155 in the pathogenesis of autoimmune arthritis in mice. *Arthritis Rheum* 2011;**63**:1281–8.
40. **Kurowska-Stolarska M**, Alivernini S, Ballantine LE, *et al*. MicroRNA-155 as a proinflammatory regulator in clinical and experimental arthritis. *Proc Natl Acad Sci U S A* 2011;**108**:11193–8.
41. **Nakasa T**, Shibuya H, Nagata Y, *et al*. The inhibitory effect of microRNA-146a expression on bone destruction in collagen-induced arthritis. *Arthritis Rheum* 2011;**63**:1582–90.
42. **Garofalo M**, Di Leva G, Romano G, *et al*. miR-221&222 regulate TRAIL resistance and enhance tumorigenicity through PTEN and TIMP3 downregulation. *Cancer Cell* 2009;**16**:498–509.
43. **Pundt N**, Peters MA, Wunrau C, *et al*. Susceptibility of rheumatoid arthritis synovial fibroblasts to FasL- and TRAIL-induced apoptosis is cell cycle-dependent. *Arthritis Res Ther* 2009;**11**:R16.
44. **Lefèvre S**, Knedla A, Tennie C, *et al*. Synovial fibroblasts spread rheumatoid arthritis to unaffected joints. *Nat Med* 2009;**15**:1414–20.

Identification of microRNA-221/222 and microRNA-323-3p association with rheumatoid arthritis via predictions using the human tumour necrosis factor transgenic mouse model

Ioannis Pandis, Caroline Ospelt, Niki Karagianni, et al.

Ann Rheum Dis 2012 71: 1716-1723 originally published online May 5, 2012
doi: 10.1136/annrheumdis-2011-200803

Notes